Simulation of moisture transport in hydrating cement-based overlay systems

Dong, Hua; Gao, Peng; Ye, Guang

Publication date
2019

Document Version
Final published version

Published in
Heron

Citation (APA)
Dong, H., Gao, P., & Ye, G. (2019). Simulation of moisture transport in hydrating cement-based overlay systems. *Heron*, *64*(1-2), 97-124.

Simulation of moisture transport in hydrating cement-based overlay systems

Hua Dong [1, 2], Peng Gao [2, 3] , Guang Ye [2]

[1] School of Materials Science and Engineering, Southeast University, Nanjing , China.

[2] Microlab, Faculty of Civil Engineering and Geosciences, Delft University of Technology, the Netherlands

[3] School of Materials Science and Engineering, South China University of Technology, Guangzhou, People's Republic of China.

Drying of cement-based overlay systems is a critical issue, because it causes differential shrinkage between the overlay material and the concrete substrate and may induce cracking or debonding of the overlay material. In this paper the mechanisms of moisture transport in hydrating cement-based overlay systems are studied. A model is proposed for simulating the moisture transport. A parameter study has been conducted to quantitatively investigate the influence of the thickness of the overlay material and the curing conditions on hydration of the overlay materials. The evolution of the moisture profile in the overlay system and the development of the degree of hydration (DOH) of the overlay material have been calculated. The change of water content in the overlay material is investigated, in terms of the water absorbed by the substrate, the water consumed by hydration of the overlay material and the water evaporated to the environment. The simulation results show that the water evaporation is a dominant factor that causes water loss of the overlay material, while the water absorption by the substrate plays only a minor role. Moist curing is much more effective than sealed curing (e.g. by using sealing agent) for hydration of the overlay material. The DOH of the overlay material is significantly increased with longer moist curing. Under the same curing condition (e.g. moist curing + drying), thinner overlay materials are more vulnerable to water loss and exhibit a lower DOH. It suggests that for proper hydration of cement-based overlay materials, moist curing is recommended rather than applying a sealing agent.

Key words: Moisture transport, cement-based overlay material, hydration, thickness, curing condition

1 Introduction

Concrete is the most widely used material in construction industry. Durability of concrete structures has been a long-standing concern [Aïtcin, 2003], [Shi, 2012]. However, the initial scatter in the quality of concrete (e.g., air voids and surface cracks) is commonly seen in practice, possibly resulting from improper mix design, poor construction practices and improper curing. Areas of concrete with poor quality may become a path for hazardous substances to penetrate into the concrete, like CO_2 and chloride ions, resulting in premature deterioration of the concrete and/or corrosion of the reinforcing steel. Cement-based overlay materials act as a physical barrier and can be used to protect the concrete structures against the attack of detrimental substances [Saricimen, 1996], [Al-Dulaijan, 2000]. However, cement-based overlay material, characterized by a small thickness (e.g. 1 or 2 centimeters), is susceptible to water loss due to evaporation or water absorption by concrete substrate. The water loss of cement-based overlay material will result in differential shrinkage between the overlay material and the substrate, and further induce cracking and de-bonding of the overlay material. The cracking of the overlay material poses negative effects on the performance of the overlay system by allowing for rapid ingress of ions (e.g. chlorides, oxygen, alkali and sulphate) [Li and Li, 2006]. To investigate the drying shrinkage-induced cracking or debonding of the overlay material, moisture transport process in the overlay system first needs to be studied and will be the topic of this work.

Change of moisture content in the overlay material is caused by hydration of the overlay material, moisture exchange between the overlay material and the concrete substrate, and moisture exchange between the overlay material and the environment. Two experimental techniques are commonly used to trace the moisture transport in cement-based overlay systems (overlay material + concrete substrate), viz. nuclear magnetic resonance (NMR) and X-ray computed tomography (CT scan) [Brocken, 1998], [Faure, 2005], [Kamyab, 2012], [Bentz and Hansen, 2000], [Lukovic and Ye, 2015]. Brocken et al. [1998] investigated moisture transport in an overlay system (fresh mortar applied on bricks) by using NMR techniques. They found that the water extraction process of the bricks was slowed down only if the bricks were almost fully saturated. Bentz and Hansen [2000] applied CT scan technique to trace moisture transport in an overlay system (fresh cement paste applied on fresh cement paste, the cement pastes had different w/c ratios). Water was found to move from the less dense to the more dense paste. Faure et al. [2005] and Kazemi-Kamyab et al.

[2012] recorded the magnetic resonance imaging profiles of an overlay system (fresh mortar applied on old concrete). They found that water in the fresh material was first absorbed by the substrate and then transferred back to the fresh material after setting. Lukovic and Ye [2015] studied moisture transport in an overlay system (fresh cement paste applied on old mortar) by using CT scan technique. They found that water loss from the repair material to the substrate led to a lower degree of hydration (DOH) of the repair material than that of the sealed-cured reference repair material. The experimental work mentioned above has presented the measured moisture profiles in the overlay systems and the DOH of the overlay materials. However, a clear understanding of the mechanisms of coupled drying and hydration process of the overlay material is still needed, which will be provided in this study.

Numerical simulation of moisture transport in cement-based material enables an convenient parameter study and helps to figure out the most influencing factors of the drying and the hydration process; by the simulation the evolution of moisture profile can be calculated [Daian, 1988], [Baroghel-Bouny, 1999], [Samson, 2005],[Ba, 2013],[Bakhshi, 2012],[Kim and Lee, 1999],[Zhang, 2009],[Zhang, 2016],[Oh, 2003]. To account for the effect of hydration of the cement-based material on the moisture transport process, various methods have been adopted [Ba, 2013], [Bakhshi, 2012], [Kim and Lee, 1999], [Zhang, 2009], [Zhang, 2016], [Oh, 2003]. For instance, the drop of relative humidity due to hydration was described as a function of porosity [Ba, 2013] or DOH [Zhang, 2009], [Zhang, 2016], [Oh and Cha, 2003]. Bakhshi et al. [2012] took the amount of bound water in the hydration products proportional to the one of free water. Kim and Lee [1999] considered the drop of relative humidity due to hydration by "assuming that the inner variation of relative humidity due to self-desiccation in drying specimens is the same as that in sealed specimens". Besides, the water consumption by hydration of cement-based materials in moisture transport process has also been considered by adapting numerical cement hydration models, e.g. HYMOSTRUC model [Oh and Cha, 2001]. However, a clear correlation between the moisture diffusivity and the evolving microstructure is still lacking, but needed for a proper simulation of moisture transport in hydrating cement-based materials. The correlation between the moisture diffusivity and the evolving microstructure will be considered in the model proposed in this study.

Efforts have also been made to simulate moisture transport in cement-based overlay systems. Brocken et al. [1998] simulated water extraction out of fresh mortar by bricks by

assuming a constant diffusivity of the mortar. A uniform moisture distribution was found in the mortar, while the moisture distribution in the bricks showed a significant gradient. This was because the bricks had lower moisture diffusivity compared with fresh mortars. In their work, only mortars in fresh state were studied, while the effect of hydration of mortars was not considered. Åhs [2007] calculated the ultimate relative humidity in sealed screed-concrete overlays, without considering time-dependent parameters (e.g. moisture diffusivity and rate of hydration). Lukovic et al. [2014] simulated moisture transport in a cement-based repair system to evaluate the drying shrinkage induced damage of the repair material. The time-dependent moisture profiles in hardened repair systems were presented. Martinola et al. [2001], [Martinola and Sadouki and Sadouki, 1998] took into consideration endogenous drying due to hydration, and simulated moisture transport in a repair system. It is noted that in the simulation of moisture transport the moisture diffusivity of overlay material changes with the hydration process. Therefore, the DOH of the overlay material has to be known since it is needed for determining the time-dependent transport property (i.e., moisture diffusivity). However, the evolution of DOH of cement-based overlay material during moisture transport in the overlay system was only rarely reported [Bentz, 2001].

In this paper the mechanisms of moisture transport in hydrating cement-based overlay systems are studied. A model is proposed to simulate the moisture transport in hydrating cement-based overlay systems. Evolution of moisture profile in the overlay systems and evolution of DOH of the overlay materials are determined. Parameter study is conducted to investigate the influence of the thickness of overlay material and the curing condition on the hydration of the overlay materials. Factors causing the water loss of the overlay materials (e.g. water absorption by the substrate and water evaporation to the environment) are discussed. Suggestions regarding the curing condition are given for a practical application of cement-based overlay materials.

2 Mechanisms of moisture transport in hydrating cement-based overlay systems

At early ages, the rate of hydration $\dot{\alpha}$ ($\dot{\alpha} = \frac{d\alpha}{dt}$, α is degree of hydration and t is time) of the overlay material strongly depends on the water content. For a proper simulation of moisture transport in hydrating cement-based overlay systems, the hydration process of the overlay material should be coupled with the moisture transport process. When

developing the model (named as Moisture-Hydration model) for simulating moisture transport in a hydrating overlay system, the following aspects have been considered separately, even though they take place simultaneously: (1) liquid water transport in the overlay material and in the substrate, (2) hydration of the overlay material, (3) vapour diffusion process in the overlay material and in the substrate, (4) Liquid water transport/vapour diffusion across the overlay material-substrate interface, (5) water evaporation from the surface of the overlay material.

2.1 Liquid water transport in a hydrating cement-based material (overlay material)

Unsaturated water flow in porous materials is often described by Richards equation [Richards, 1931].

$$\frac{d\theta}{dt} = div\left(k \cdot grad\ p(\theta)\right) \tag{1}$$

Where θ is the water content in the material, k is the water permeability of the material and $p(\theta)$ is the capillary pressure.

The water content θ can be substituted by the water saturation level s. The water saturation level is calculated with $s = \theta / (\rho_w \cdot \phi)$, where ρ_w is the density of water, ϕ is the porosity of the material. By introducing the relative permeability $k(s)$ of the material [Baroghel-Bouny, 2007], Eq. (1) becomes:

$$\frac{\partial(\phi \cdot s)}{\partial t} = div\left(\frac{-K}{\mu} \cdot k(s) \cdot grad\ p(s)\right) \tag{2}$$

where K is the intrinsic permeability of the porous material, $k(s)$ is relative water permeability of porous material with a water saturation level s and μ is the dynamic viscosity of water.

To account for the water consumed by hydration of the overlay material, a sink term W_{hyd} is introduced. Determination of W_{hyd} will be given in section 2.2. Considering the transformation of water from liquid phase to vapour phase, $W_{l\to v}$, water transfer through a hydrating cement-based material can be described by:

$$\frac{\partial(\phi \cdot s)}{\partial t} = div\left(\frac{-k}{\mu} \cdot k(s) \cdot \frac{dp(s)}{ds} \cdot grad\ s\right) - W_{hyd} - W_{l\to v} \tag{3}$$

The quantities preceding the gradient within the parenthesis can be lumped together to form a moisture diffusivity:

$$D_l(s) = \frac{-K}{\mu} \cdot k(s) \cdot \frac{dp(s)}{ds} \tag{4}$$

In this study, Eq. (3) is used to describe the movement of liquid water in the materials under isothermal conditions. The water saturation level dependency of $k(s)$ and $p(s)$ are described by the van Genuchten (VG) model [Van Genuchten, 1980].

$$p(s) = a \cdot (s^{-1/m} - 1)^{1-m} \tag{5}$$

$$k(s) = s^{0.5} \cdot (1 - (1 - s^{1/m})^m)^2 \tag{6}$$

where a and m are two parameters. Determination of these parameters will be presented in section 3.3).

2.2 *Hydration of cement-based materials with arbitrary water content*

The term W_{hyd} in Eq. (3) refers to the water consumed by hydration and has to be formulated for simulating moisture transport in hydrating overlay systems. At complete hydration, 1 g of cement chemically binds approximately 0.23 g of water [Jensen and Hansen, 2001]. W_{hyd} can be determined according to Eq. (7).

$$W_{hyd} = \frac{0.23 \cdot m_{cem} \cdot \dot{\alpha}}{\rho_w} \tag{7}$$

where $\dot{\alpha}$ is the rate of hydration and calculated with $\dot{\alpha} = \frac{d\alpha}{dt}$, α is the DOH, m_{cem} is the mass of cement in a unit volume of cement paste and ρ_w is the density of liquid water.

For a cement paste, the rate of hydration $\dot{\alpha}$ depends primarily on the amount of water that is available for hydration. According to Van Breugel [1991], only capillary water is available for the hydration of cement, while water in gel pores of C-S-H does not contribute to the hydration. The rate of hydration $\dot{\alpha}$ of a cement-based material can be determined by using a modified version of HYMOSTRUC3D model [Van Breugel, 1991], [Koenders, 1997].

2.3 *Water vapour diffusion through cement-based materials*

According to Ho and Webb [2006], the flux of water vapour in a clear fluid can be described as:

$$F_v = -\rho_g \cdot D_{v-g} \cdot grad\ \omega_v \tag{8}$$

where ρ_g is the density of the gas, D_{v-g} [m²/s] is the diffusion coefficient of water vapour in the gas, and ω_v is the mass fraction of water vapour in the gas.

To transform the mass fraction of water vapour in the gas ω_v into the mass of water vapour in a unit volume of gas, the term w_v [kg/m³] is introduced, with the form of $w_v = \rho_g \omega_v$. Eq. (8) is rewritten as:

$$F_v = -D_{v-g} \cdot grad\ w_v \tag{9}$$

In this study the gas pressure in the pore structure is assumed to be equal to the atmospheric pressure. The convection of air in the pore system of the material is neglected. The mass flux of water vapour through a porous material, J_v , can be described as:

$$J_v = \phi_g \cdot v_v = -F(s) \cdot D_{v-g} \cdot grad\ w_v \tag{10}$$

where ϕ_g is the volume fraction of gas-filled pores, with $\phi_g = \phi \cdot (1-s)$ $\cdot v_v$ is the velocity of water vapour, $F(s)$ is the resistance factor and calculated with $F(s) = \phi^{4/3} \cdot (1-s)^{10/3}$ [Millington and Quirk, 1961].

When the liquid-vapour phase transition of water is considered, the vapour diffusion through a porous material is described by:

$$\frac{\partial(\phi_g \cdot w_v)}{\partial t} = div\left(-F(s) \cdot D_{v-g} \cdot grad\ w_v\right) + W_{l \to v} \tag{11}$$

The vapour diffusivity $D_v(s)$ can be defined as:

$$D_v(s) = -F(s) \cdot D_{v-g} \tag{12}$$

2.4 *Liquid water – vapour phase transition*

During moisture transport in a cement-based material, phase transition between liquid water and water vapour always takes place in the pore space in order to maintain the liquid-vapour equilibrium [Baroghel-Bouny, 1999]. In cement-based materials, phase transition is assumed to be very fast in the pores, because the pore sizes are mostly below several microns. It is believed that liquid water and water vapour in a small portion of pore space are always in a state of equilibrium [Shimomurat and Maekawa, 1997]. The phase transition is calculated by combining the Kelvin equation and the Young-Laplace equation [Adamson and Gast, 1967].

2.5 *Liquid water transport/vapour diffusion across the overlay material-substrate interface*

During moisture transport in an overlay system, mass conservation of moisture at the interface between overlay material and substrate should be dealt with care [Szymkiewicz, 2012], [Nurge, 2010]. Usually, the microstructure of the overlay material is different from that of the substrate. During the moisture transport, two criteria are used to fulfil water mass conservation across the interface. The first one is that the capillary pressure p of each interface node should be the same (Eq. 13). Another criterion is that the incoming moisture flux towards one material should be equal to the outgoing flux from the other material. The flux of liquid water J_s ($J_s = -D_l(s) \cdot grad\ s$) at the overlay material-substrate interface follows Eq. (14). Similarly, the vapour flux J_v ($J_v = -D_v(s) \cdot grad\ w_v$) at the overlay material-substrate interface follows:

$$p(s_{c0}) = p(s_{s0}) \tag{13}$$

$$J_s(s_{c0}) = J_s(s_{s0}) \tag{14}$$

$$J_v(w_{v_{c0}}) = J_v(w_{v_{s0}}) \tag{15}$$

where s_{c0} and s_{s0} are the water saturation levels of the interface nodes of the overlay material and the substrate, respectively. $w_{v_{c0}}$ and $w_{v_{s0}}$ are the mass of water vapour of the interface nodes of the overlay material and the substrate, respectively.

2.6 *Water evaporation on the surface of an overlay system*

Water evaporation is a process by which water is transferred from the surface of material to the atmosphere. It is well know that evaporation is an endothermic process, in which heat is absorbed. In this study, isothermal condition is considered. A theoretical moisture

flux through material surface is simulated in this study. It allows for conserving the mass of water through the exposed surface of the material. To account for different curing regimes, boundary condition is applied at a distance from the exposed surface.

Under an isothermal condition, water evaporation from the surface of a material is only driven by the gradient of vapour content w_v at the 'liquid water surface'. According to Fick's first law, the moisture flux in the gas J_a [kg/(m² s)] is given by:

$$J_a = -D_{v-g} \cdot grad\, w_v \tag{16}$$

The vapour content in the gas w_v [kg/m³] can be calculated with $w_v = \mathrm{RH} \cdot w_{sat}$, where RH is the relative humidity in the gas. The diffusion coefficient of the water vapour in the air, D_{v-g}, can be taken as 2.42×10^{-5} m²/s at 20 °C and 1 atm [Wiederhold, 1997].

When water evaporation takes place on the surface of a porous material, J_s ($J_s = -D_l(s) \cdot grad\, s$) or J_a ($J_a = -D_{v-g} \cdot grad\, w_v$) can describe the moisture flux at the interface between the material and the atmosphere. At the interface, it holds:

$$\rho_w \cdot D_l(s) \cdot grad\, s = D_{v-g} \cdot grad\, w_v \tag{17}$$

By assembling equations described in section 2, a Moisture-Hydration model for simulating moisture transport in a hydrating cement-based overlay system is completed.

3 Quantification of parameters

In this study, fresh overlay material (i.e., cement paste) is applied on a 1-year old concrete substrate. The microstructure of the overlay material may change due to hydration, while no further hydration of the substrate is considered. To simulate moisture transport in the overlay system, a couple of parameters (e.g. the porosity and the rate of hydration) and properties (i.e. the intrinsic permeability and the moisture isotherm) of the overlay material should be determined first.

In the Moisture-Hydration model, the moisture diffusivity (Eq. 4) and the vapour diffusivity (Eq. 12) of the cement paste are described with a number of parameters, viz. the porosity ϕ, the intrinsic permeability K and the parameters (e.g. a and m in Eq. 5 and Eq. 6) in van Genuchten model. All these parameters are determined by the microstructure of the materials and can be related to the DOH α.

3.1 *Porosity* (ϕ_{cap} , ϕ_{gel} and ϕ)

In cement pastes, capillary pores are the residual unfilled space between cement particles. Gel pores are entirely contained within C-S-H [Jennings and Tennis, 1994]. The capillary pores refer to the pores larger than 10 nm, while gel pores refer to the pores smaller than 10 nm [Mindess, 2003]. In this study, the capillary porosity ϕ_{cap} of the cement paste is calculated based on the DOH α [Van Breugel, 1991]. The gel porosity ϕ_{gel} is determined following the methodology proposed in the literature [Jennings, 2008], [Tennis and Jennings, 2000], [Taylor, 1987], taking into account the amounts of high-density and low-density C-S-H gels.

3.2 *Intrinsic permeability K*

In order to study the moisture transport in a hydrating cement paste, the intrinsic permeability of the cement paste (from casting to hardening) should be described as a function of the DOH α.

Permeability of hardened cement pastes has been studied experimentally [Powers, 1954], [Nyame, 1979], [Banthia and Mindess, 1989]. Note that most experimental work is focused on relatively mature cementitious materials (i.e. cement pastes with at least 1 day curing [Banthia and Mindess, 1989]), because the permeability of cementitious materials at very early ages is hard to measure due to the fast hydration process of the materials.

Simulation of 3D fluid flow in digital microstructures of cement pastes allows the computation of certain inherent characteristics (i.e. intrinsic permeability K), and thus, may overcome the difficulty in laboratory measurements. In this study, the digital microstructures of early age cement pastes are generated by HYMOSTRUC3D model, with dimensions of $100 \times 100 \times 100$ μm^3 and a digital resolution of 0.5 μm/voxel. Water flow through the digital microstructures is simulated using the Lattice Boltzmann Method [McNamara and Zanetti, 1998]. Then the intrinsic permeability of early age cement pastes (e.g. age < 1 day) is determined according to Darcy's law. Intrinsic permeability of cementitious materials at late ages (e.g. age ≥ 5 days) is determined by using an empirical equation that describes the relationship between water permeability and curing age [Nyame, 1979]. The intrinsic permeability of the cement paste is plotted against the DOH. For cement paste with a curing age between 1 day and 5 days, the intrinsic permeability is obtained by spline interpolation.

3.3 Moisture isotherm (Parameters in van Genuchten model)

For the simulation of moisture transport in hydrating overlay systems, the parameters (i.e. a and m) in the Van Genuchten model (Eq. 5 - Eq. 6) have to be determined and described as a function of the DOH. These parameters (i.e. a and m) are obtained by fitting the capillary pressure-water saturation curves to Eq. 5. The capillary pressure-water saturation curves can be deduced from the moisture isotherm according to the Kelvin equation and the Young-Laplace equation [Adamson, 1967]. The moisture isotherm describes the relationship between water content and equilibrium relative humidity of a material at a constant temperature.

Moisture isotherms of cement pastes can be determined experimentally. Absorption isotherms of hardened cement pastes with the curing time longer than 7 days are available in literature [Baroghel-Bouny, 2007], [Saeidpour and Wadsö, 2015], [Powers and Brownyard, 1946]. Xi et al. [1994] proposed an empirical model to predict the absorption isotherms of hardened cementitious materials. In their model, the age of the materials is no less than 5 days.

The determination of moisture isotherm becomes difficult for early age cement pastes, because the microstructures of the cement pastes change with the ongoing hydration, and the determination of the moisture isotherm is usually time-consuming [Aligizaki, 2005]. A long duration of testing will vitiate the moisture isotherms. Alternatively, numerical models have been proposed to determine capillary pressure-water saturation curves of a porous media or moisture isotherms of cementitious materials, e.g. pore network model [Ranaivomanana, 2013], model based on Lattice Boltzmann method [Zalzale and McDonald, 2012] and model based on Level Set Method [Prodanovic and Bryant, 2006].

In this study, to determine the capillary pressure-water saturation curves of early age cement pastes (e.g. age < 1 day), displacement of water by air (i.e. desorption process) in a saturated cement paste at a particular capillary pressure is simulated using a Level Set Method [Prodanovic and Bryant, 2006]. The same digital microstructure of the cement paste generated by HYMOSTRUC3D as for LBM simulation is used in the simulation of desorption process. For later age cement pastes (e.g. age ≥ 5 days), the capillary pressure-water saturation curves are deduced from the moisture isotherm (absorption). The moisture isotherms of late age cement pastes are determined using an empirical model [Xi, 1994]. Then the parameters (i.e. a and m) in the Van Genuchten model (Eq. 5 - Eq. 6) of

early age (e.g. age < 1 day) and late age (e.g. age ≥ 5 days) cement pastes are determined by curve fitting and plotted against the DOH. For cement paste with a curing age between 1 day and 5 days, the parameters (i.e. a and m) in the Van Genuchten model are obtained by spline interpolation. Note that the desorption isotherm and the absorption isotherm should be used for determining the parameters in the Van Genuchten model for describing the drying process and the wetting process of cement-based materials, respectively. However, in this study it is hypothesized that both wetting and drying processes can be described using the same parameters (i.e., parameters determined from desorption isotherm for early age cement-based materials, and absorption isotherm for later age cement-based materials).

4 Simulation of moisture transport in hydrating cement-based overlay systems

When a cement-based overlay material is applied on a concrete substrate, moist curing is normally required for a certain period of time to ensure a proper hydration process of early age overlay materials. The moist curing is also beneficial to prevent plastic shrinkage-induced cracking at early ages due to rapid water loss from the material [Mindess, 2003]. After a period of moist curing the overlay system can become subjected to drying. The moisture starts to evaporate from the overlay material to the environment. Meanwhile, the moisture exchange takes place between the overlay material and the substrate. Consequently, differential drying shrinkage of the overlay material and the substrate develops over time, which increases the probability of cracking and/or debonding of the overlay material.

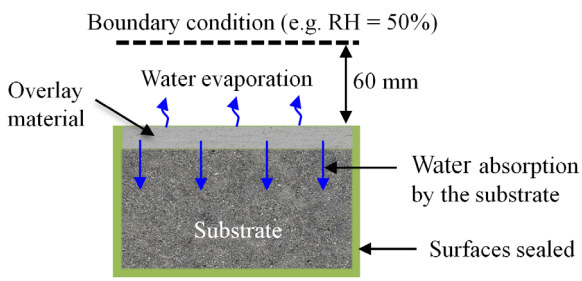

Figure 1: A typical scenario of moisture transport in an overlay system. The boundary condition is applied at a distance of 60 mm above the surface of the overlay material to account for different curing conditions.

One-dimensional (1D) simulation of moisture transport in the overlay system is considered. The top surface of the overlay system is subjected to various curing conditions, while the bottom surface of the substrate is always sealed (Figure 1). The moisture profile in the overlay system and the DOH of the overlay material are calculated. The influence of several parameters on the moisture transport is evaluated, viz. the thickness of overlay material and the duration of different curing conditions.

4.1 Materials of overlay systems for the simulation of moisture transport

4.1.1 Overlay material-mixture composition

The overlay material is a cement paste (w/c = 0.3). Ordinary Portland cement CEM I 42.5N is used. The mineral composition of the cement (by mass) is C_3S : C_2S : C_3A : C_4AF = 53.5% : 21% : 7.5% : 10.7% [Van Breugel, 1991]. It should be noted that mortar is commonly used as concrete overlay material, rather than the cement paste. The purpose of using the cement paste as an overlay material in this study is to simplify the investigation of moisture transport in the overlay system, considering the hydration process and formation of microstructure of the overlay material.

4.1.2 Substrate

The substrate is 1 year-old concrete (w/c = 0.48). The total porosity of the substrates is 12.2%. Detailed characteristics of the substrates can be found in [Baroghel-Bouny, 1999]. Further hydration of concrete substrate after the application of overlay material is neglected. The thickness of the substrates is 50 mm. Note that, in practice the thickness of concrete elements are usually larger than 50 mm. The thickness of 50 mm is chosen in this study for a fast numerical computation, and considered large enough for the parameter study of moisture transport in the overlay system.

4.2 Exposure scenarios of the overlay systems and parameters to be evaluated

Moisture transport in overlay systems is simulated for different thicknesses of overlay materials (i.e. 6, 10 and 20 mm). In order to investigate the role of the curing regime in the moisture distribution in the overlay systems and the DOH of the overlay materials, different curing regimes (e.g., moist curing or sealed curing followed by drying under 50% RH) are applied to the overlay systems (Table 1). When the overlay system is subjected to drying, a Dirichlet boundary condition (i.e., RH = 50%) is applied at a distance of 60 mm

above the surface of the overlay material. This distance has been validated based on experimental results in [Baroghel-Bouny, 1999], [Snyder and Bentz, 2004].

Table 1: Description of the reference cement paste and the overlay systems

Reference cement paste(1)	Thickness of overlay material [mm]	Curing regime (T = 20°C) Sealed until 14 days
C06-Moist1d	6	1 d moist + 13 d 50% RH
C10-Moist1d	10	1 d moist + 13 d 50% RH
C20-Moist1d	20	1 d moist + 13 d 50% RH
C10-Moist3d	10	3 d moist + 11 d 50% RH
C10-Moist7d	10	7 d moist + 7 d 50% RH
C10-Sealed1d	10	1 d sealed +13 d 50% RH(2)
C10-Sealed3d	10	3 d sealed +11 d 50% RH
C10-Sealed7d	10	7 d sealed +7 d 50% RH

(1) The reference cement paste is made of Portland cement CEM I 42.5N with a w/c of 0.3.
(2) The sealed curing simulates the use of a curing compound on the surface of the overlay material.

*4.3 **Simulation results and discussion***

In this section the simulated evolution of moisture profiles in the overlay systems (Table 1) and the evolution of DOH of the overlay materials are presented and discussed. The simulated results are compared with those of the reference cement paste (w/c = 0.3, fully sealed). The water loss of the overlay material is investigated, with respect to the water consumed by hydration, the water absorbed by the substrate and the water evaporated to the environment.

4.3.1 Effect of the thickness of overlay material (6, 10 and 20 mm) on moist transport in the overlay systems and on hydration of the overlay materials

(a) Moisture profile in the overlay system with a 10 mm-thick overlay material

Figure 2 presents the moisture profiles in the overlay system with a 10 mm-thick overlay material. After the application of the overlay material, the substrate immediately starts absorbing water from the overlay material. During 1 day moist curing, the overlay material still remains saturated with water. After 1 day, the overlay material is exposed to a RH of 50%. The water saturation level in the overlay material decreases drastically, due to the

continuing water absorption by the substrate and the water evaporation to the environment. Meanwhile, hydration of the overlay material consumes some amount of water. An almost uniform water loss is observed over the thickness of the overlay material. This phenomenon can be explained by the fact that the moisture moves rapidly in a young overlay material with a highly connected pore system. Similar results have been reported by Selih et al. [1996] and Bentz et al. [2001].

After 3 days, the water saturation level in the 10 mm-thick overlay material has dropped below 60%, which is lower than that (> 80%) in the reference cement paste. Distinct difference in water saturation level can be clearly seen from the overlay material-substrate interface (Figure 2b). The water saturation level of the substrate at the interface remains higher than 70% at 14 days, while the water saturation level in the overlay material becomes lower than 5% at 14 days. It can be explained by the difference in the microstructures of the overlay material and the substrate. The decrease of the water saturation level will affect the hydration process of the overlay material, which will be discussed below.

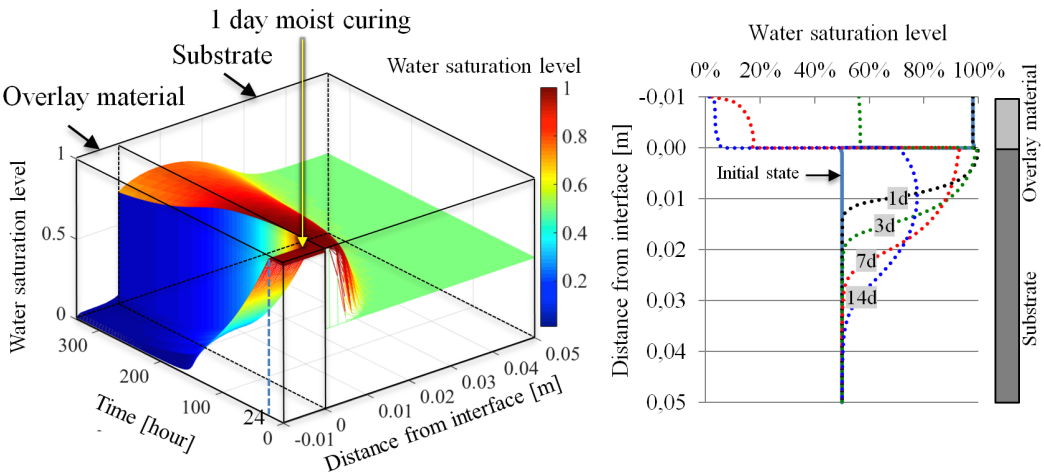

(a) 3D plot *(b) 2D plot*

Figure 2: Calculated moisture profiles in the overlay system C10-Moist1d (Table 1). A 10 mm-thick overlay material (w/c = 0.3) is applied on the substrate. One of day moist curing is applied, followed by exposure to 50% RH until 14 days.

(b) Evolution of water content and development of degree of hydration of the overlay materials with different thicknesses (6, 10 and 20 mm)

Figure 3a presents the evolution of the average water content θ ($\theta = s \cdot \rho_w \cdot \phi$) in the overlay materials with different thicknesses (i.e. 6, 10 and 20 mm). After 1 day moist curing, the water content θ in the thicker overlay material (e.g. 20 mm) is higher than that in thinner overlay materials (6 or 10 mm). The water content in the 6 mm-thick overlay material and the 10 mm-thick overlay material decreases to about 0, which is lower than expected. This can be explained by the relative low value of DOH of the thin overlay material after drying for a period of time. The overlay material with a lower value of DOH has a coarser microstructure, which lead to a lower water content at RH = 50%. The evolution of the DOH of the overlay materials is depicted in Figure 3b. There is no difference of the DOH between the overlay materials during 1 day moist curing. After the overlay materials are exposed to a RH of 50%, the DOH curves of the overlay materials start to diverge. An earlier cease of hydration is seen for a thinner overlay material (i.e. 6 mm overlay material).

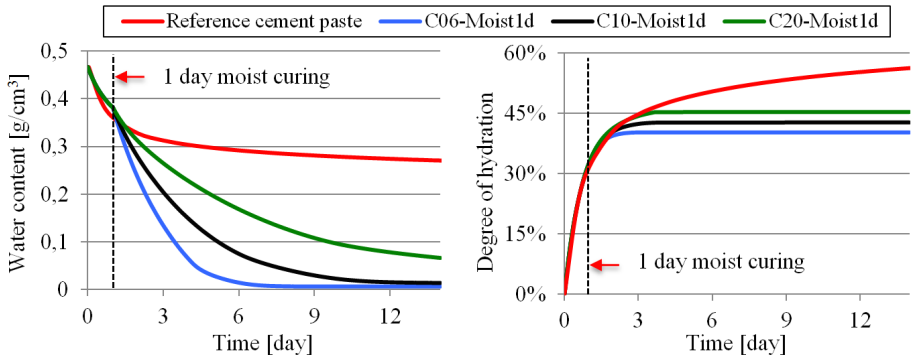

(a) Water content *(b) Degree of hydration*

Figure 3: Calculated evolution of water content and degree of hydration of the overlay materials (w/c = 0.3) with different thicknesses (6, 10 and 20 mm). The overlay materials are applied on the substrate. One day moist curing is applied, followed by exposure to 50% RH until 14 days. The reference cement paste is fully sealed.

By comparing the DOH of the overlay materials with that of the reference cement paste, the combined effect of the water evaporation and the water absorption by the substrates on the hydration of overlay materials is evaluated. The hydration process of the overlay materials (curing condition: 1 d moist curing followed by 13 d 50% RH) has almost ceased

after 4 days due to drying, while the reference cement paste continues to hydrate. Figure 4 shows the DOH of the overlay materials with different thicknesses at 14 days. The overlay material with a larger thickness has a higher DOH at 14 days. It can be concluded that the thickness of overlay material has a noticeable influence on the hydration process of an overlay material. A thinner overlay material is more susceptible to lose its water when it is applied on the absorptive substrate and exposed to a dry environment (e.g. RH = 50%). The greater water loss results in a lower DOH and indicates a higher permeability of the overlay materials.

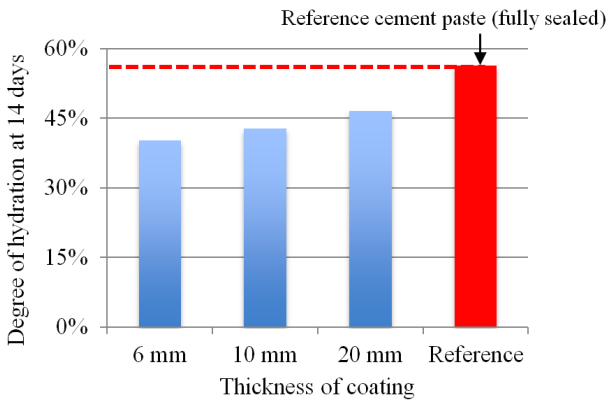

Figure 4: Calculated average degree of hydration at 14 days of the overlay materials (w/c = 0.3) with different thicknesses (6, 10 and 20 mm). The overlay materials are applied on the substrate. One day moist curing is applied, followed by exposure to 50% RH until 14 days. The reference cement paste is fully sealed.

4.3.2 *Effect of curing regime on moist transport in the overlay systems and on the hydration of the 10 mm-thick overlay materials*

As described in section 4.2, after application of the 10 mm-thick overlay materials, various curing regimes are applied to the overlay systems:

- Moist curing (1, 3, and 7 days), followed by exposure to 50% RH until 14 days
- Sealed curing (1, 3, and 7 days), followed by exposure to 50% RH until 14 days

(a) Moisture profiles in overlay systems under various curing regimes

In this section moisture profiles in 2 typical overlay systems (C10-Moist3d and C10-Seaeld3d) are presented to illustrate the influence of curing regimes on moisture transport in overlay systems.

3 days moist curing: C10-Moist3d

In C10-Moist3d, 3 days moist curing is applied to the overlay system after application of the overlay material. Figure 5 presents the moisture profile in the overlay system. After 14 days the water saturation level of the overlay material becomes low ($s < 20\%$), but is higher than that ($s < 5\%$) in the overlay material with 1 day moist curing (Figure 2b). Longer moist curing provides more water for the hydration of the overlay material.

3 days sealed curing: C10-Sealed3d

Figure 6 presents the moisture profiles in the overlay system with 3 days sealed curing followed by exposure to 50% RH until 14 days. Immediately after application of the overlay material, the water saturation level in the overlay material starts to decrease because of the hydration of the overlay material and the water absorption by the substrate. After 3 days sealed curing and exposure to an ambient RH of 50%, water starts to evaporate from the surface of the overlay material, causing a drastic decrease of the water saturation level in the overlay material. The water saturation level in the overlay material with 3 days sealed curing (Figure 6) is much lower compared to the overlay material with 3

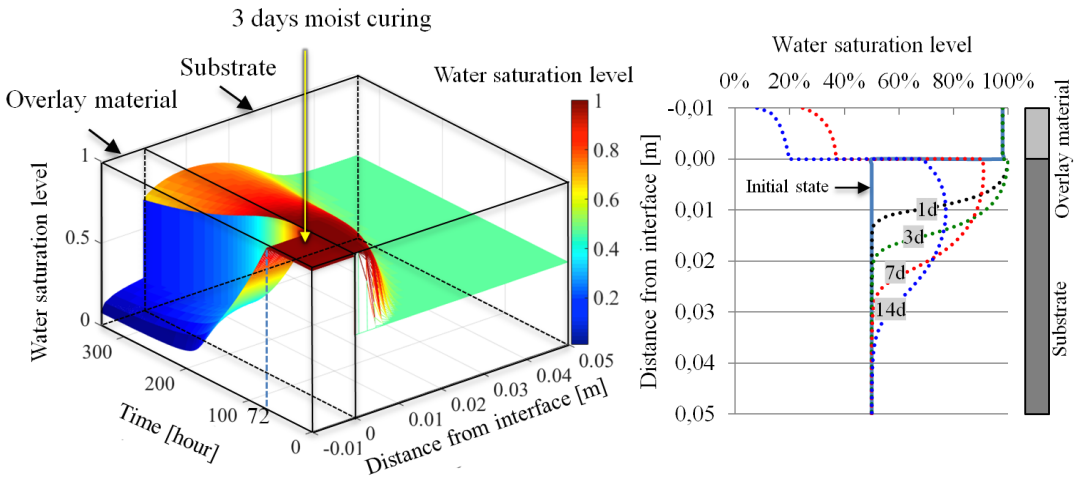

(a) 3D plot *(b) 2D plot*

Figure 5: Calculated moisture profiles in the overlay system C10-Moist3d (Table 1). A 10 mm-thick overlay material (w/c = 0.3) is applied on the substrate (s = 50%). Three days moist curing is applied, followed by exposure to 50% RH until 14 days.

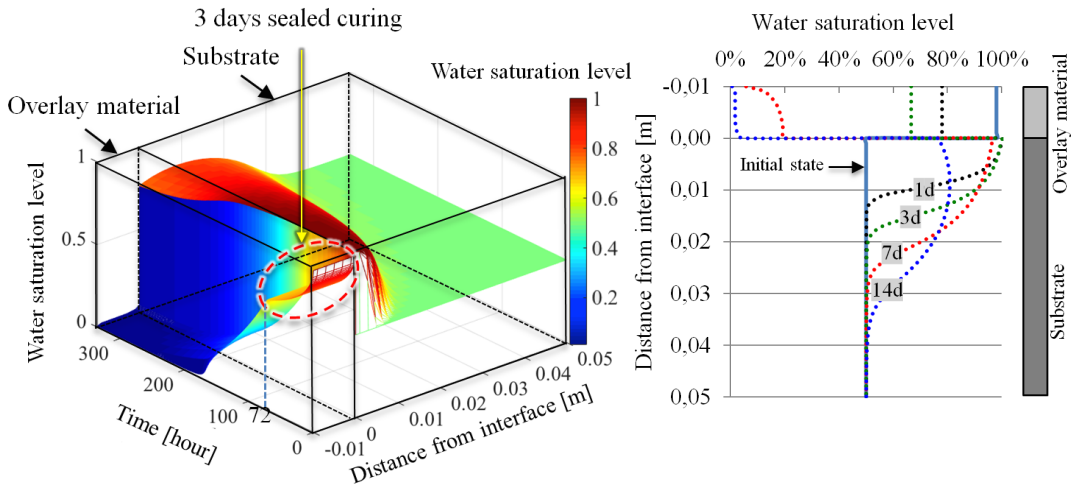

(a) 3D plot *(b) 2D plot*

Figure 6: Calculated moisture profiles in the overlay system C10-Sealed3d (Table 1). A 10 mm-thick overlay material (w/c = 0.3) is applied on the substrate (s=50%). Three days sealed curing is applied, followed by exposure to 50% RH until 14 days.

(b) Evolution of water content and development of degree of hydration of overlay materials under various curing regimes

Overlay materials moist-cured for 1, 3 or 7 days, followed by exposure to RH = 50%

Figure 7a presents the evolution of the water content in the overlay materials with moist curing. The water content in a 10 mm-thick overlay material highly depends on the period of moist curing. With longer moist curing, the water content in the overlay material is much higher. The water content in the overlay materials is compared to that in the reference cement paste. During the moist curing (1, 3 or 7 days), the water content in the overlay material is higher than that in the reference cement paste. After the overlay materials are exposed to RH = 50%, the water content in the overlay materials decreases drastically due to the water evaporation to the environment and the water absorption by the substrate, and becomes lower than that in the reference cement paste.

Figure 7b presents the evolution of the average DOH of overlay materials under moist curing. The hydration of the overlay materials is significantly affected by the duration of moist curing. With longer moist curing, the DOH of the overlay material is noticeably higher than that with a shorter moist curing.

Overlay materials sealed-cured for 1, 3 or 7 days, followed by exposure to RH = 50%

Figure 8 presents the evolution of the water content and the average DOH of the overlay materials with sealed curing. After application of the overlay materials, the top surfaces of the overlay materials were sealed. From the figure it can be seen that the overlay materials have lower water content than the reference cement paste. This can be explained by the water absorption by the substrates. Overlay materials with longer sealed curing exhibit

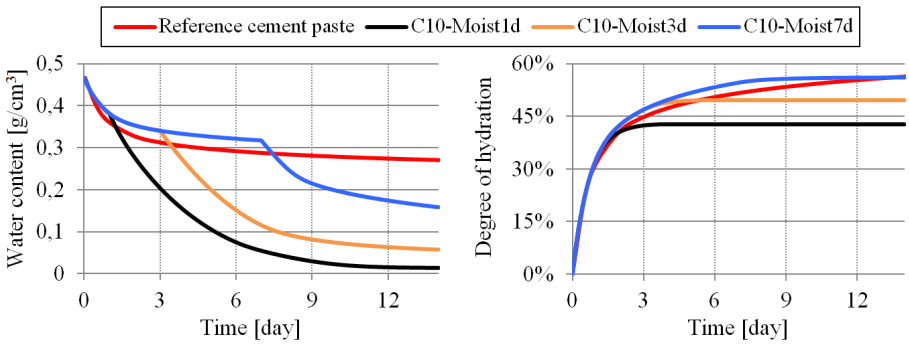

(a) Water content *(b) Degree of hydration*

Figure 7: Calculated water content and average degree of hydration of the 10 mm-thick overlay materials (w/c = 0.3) applied on the substrate, and exposed to different curing regimes (1, 3 or 7 days moist curing, followed by exposure to RH = 50% until 14 days). The reference cement paste is fully sealed.

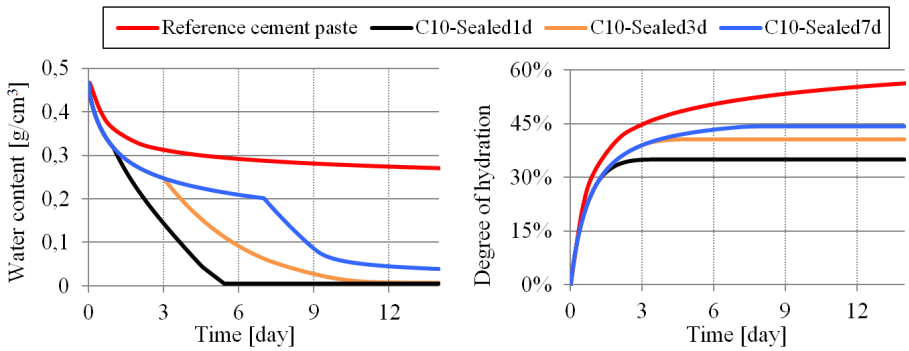

(a) Water content *(b) Degree of hydration*

Figure 8: Calculated water content and average degree of hydration of the 10 mm-thick overlay materials (w/c = 0.3) applied on the substrate, and exposed to different curing regimes (1, 3 or 7 days sealed curing, followed by exposure to RH = 50% until 14 days). The reference cement paste is fully sealed.

higher water content and higher DOH. Moreover, the overlay materials with sealed curing have lower water content and lower DOH than those with moist curing (Figure 7). It suggests that moist curing is essential for the hydration of overlay materials.

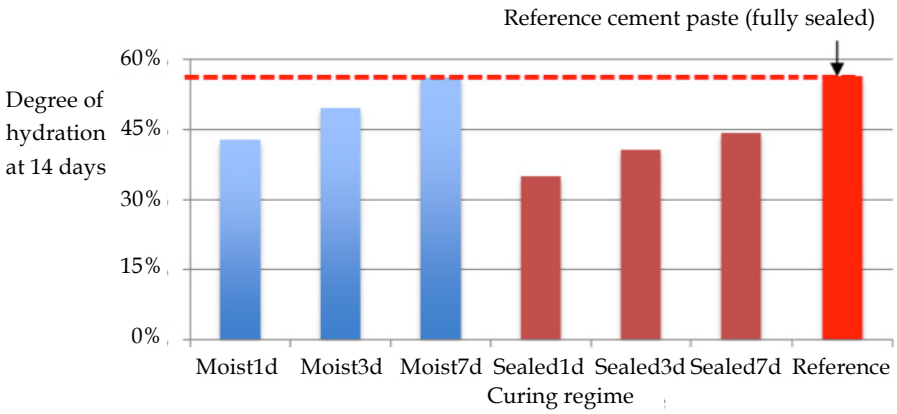

Figure 9: Calculated average degree of hydration of the 10 mm-thick overlay materials (w/c = 0.3) at 14 days. The overlay materials are applied on the substrate. The top surfaces of the overlay materials are sealed or subjected to moist curing for 1, 3 or 7 days, followed by exposure to RH = 50% until 14 days. The reference cement paste is fully sealed.

4.3.3 Investigation of water loss of the 10 mm-thick overlay material (C10-Moist3d: 3 days moist curing, followed by exposure to RH = 50% until 14 days)

After an overlay material is applied on concrete substrate, water in the overlay material may be either absorbed by the substrate and/or evaporate to the environment. The water loss affects the hydration process of the overlay material. This section presents the evolution of water content in a typical overlay system (C10-Moist3d), including the total amount of water in the overlay material and the amount of water that is available for hydration. Besides, water loss due to the absorption by the substrate and the evaporation to the environment is also discussed.

Figure 10a shows the average water saturation level in the overlay material. During 3 days moist curing, the overlay material remains saturated. After 3 days, the overlay system is exposed to the 50% RH, the water saturation level of the overlay material drops gradually, which is mainly due to water evaporation.

In the overlay material, the water content θ is calculated as the sum of capillary water and gel water. As described in section 2.2, only capillary water is available for the hydration of cement, while water in gel pores of C-S-H doesn't contribute to hydration. The amount of capillary water $\theta_{cap}(t)$ changes during the hydration process, and can be calculated with:

$$\theta_{cap}(t) = \rho_w \cdot \left(\phi(t) \cdot s(t) - \phi_{gel}(t)\right) \tag{18}$$

where ρ_w is the density of water, $\phi(t)$ is the total porosity of the overlay material, $s(t)$ is the water saturation level and $\phi_{gel}(t)$ is the gel porosity.

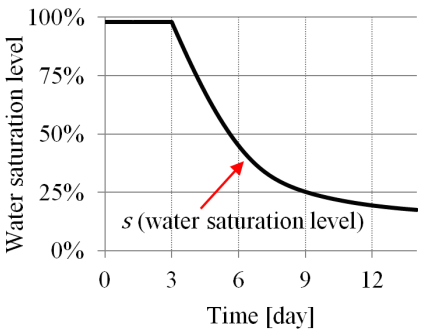

(a) Average water saturation level in overlay material

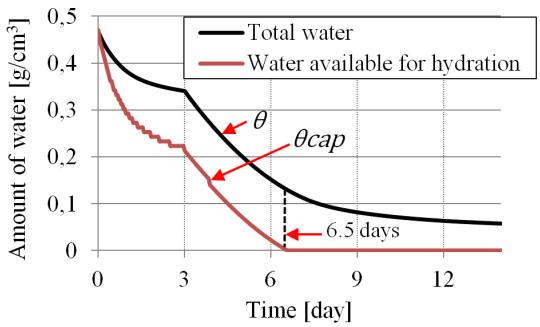

(b) Amount of water in the overlay material

Figure 10: Calculated average water saturation level and amount of water in the overlay material in C10-Moist3d. A 10 mm-thick overlay material (w/c = 0.3) is applied on the substrate. Three days moist curing is applied, followed by exposure to RH = 50% until 14 days.

Figure 10b shows the total amount of water and the amount of water in capillary pores in the overlay material. As the hydration proceeds, water is gradually consumed. The amount of capillary water available for the hydration decreases. The overlay material loses all the capillary water after 6.5 days, and the hydration has almost ceased. However, drying of the overlay material still proceeds, in which process the water in gel pores is gradually lost. The drying of the overlay material in the overlay system is indicated by the decrease of total water content θ.

To further investigate the role of the substrate and the environment in the hydration of the overlay materials, the amounts of water absorbed by the substrate and water evaporated to the environment are calculated. Figure 11 shows the water loss from the overlay materials,

together with the amount of water consumed by hydration. After application of the overlay material, the substrate immediately absorbs water from the overlay material (red lines). After 3 days moist curing, the overlay system is exposed to 50% RH. Water starts to evaporate from the overlay material to the environment (blue lines). After 6 days, the substrate stops absorbing water from the overlay material and starts losing water. Both the water absorption by the substrates and the evaporation of water may affect the hydration process of the overlay materials. The absorption by the substrate mostly takes place during 3 days moist curing. However, the water absorption by the substrate can hardly affect the hydration of the overlay materials, because the overlay materials remain saturated during moist curing. After 3 days moist curing the dominant factor of water loss of the overlay materials is water evaporation, while the water absorption by the substrates plays only a minor role.

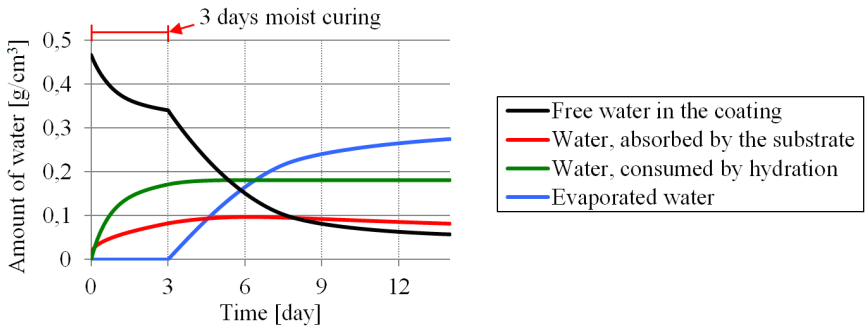

Figure 11: Calculated water loss of the overlay material applied on substrate (C10-Moist3d). The 10 mm-thick overlay material is applied on ordinary concrete substrate. Three days moist curing is applied, followed by an exposure to RH = 50% until 14 days

5 Conclusion

The mechanisms of moisture transport in hydrating overlay systems were studied. A model was proposed to simulate the moisture transport, taking into account liquid water transport, water vapour diffusion in the overlay system and hydration of the overlay material. Parameter study is conducted to investigate the influence of the thickness of overlay material and curing condition on the hydration of the overlay material applied on concrete substrate. The evolution of moisture profile in the overlay system and the development of DOH of the overlay material are calculated. The change of water in the overlay material is investigated, in terms of water absorbed by the substrate, water

consumed by hydration of the overlay material and water evaporated to the environment. The following conclusions can be drawn:

- Moist curing is much more effective than sealed curing (e.g. by using sealing agent) for the hydration of the overlay materials. For the hydration of the 10 mm-thick overlay material, 1 day moist curing is almost equivalent to 7 days sealed curing. With 7 days moist curing + 7 days exposure to 50% RH, the DOH of the overlay material is comparable with that of a reference cement paste fully sealed for 14 days. Longer moist curing is essential to compensate for water absorption by the substrates, and for ensuring a proper hydration process of the overlay material. For a proper hydration of the overlay materials, moist curing is suggested, rather than applying a sealing agent.

- Under the same curing condition (e.g. moist curing + drying), thinner overlay materials are more vulnerable to water loss and exhibit lower DOH. It indicates that moist curing is essential especially for hydration of thin overlay materials.

- After exposure to drying condition, water evaporation from the overlay material is a dominating factor that causes the drying of overlay material, while the water absorption by the substrate plays only a minor role.

- For further study of drying shrinkage-induced cracking/debonding of the overlay material, moisture content and mechanical properties of the overlay material and the substrate should be known. The mechanical properties, e.g. elastic modulus and tensile strength, can be related to the DOH of the materials obtained by the simulation in this study. Therefore, this study provides information for further study of drying shrinkage-induced cracking/debonding of the overlay material.

Acknowledgement

This work was supported by the Dutch Technology Foundation (STW) [grant number 10981].

References

Adamson, A.W. and Gast, A.P. (1967). *Physical chemistry of surfaces*, Interscience, New York.

Åhs, M. (2007) Moisture redistribution in screeded concrete slabs, Report TVBM 3136.

Aïtcin, P.C. (2003). The durability characteristics of high performance concrete: A review, *Cem Concr Compos*, 25: 409-420.

Aligizaki, K.K. (2005). *Pore structure of cement-based materials: testing, interpretation and requirements*, CRC Press.

Al-Dulaijan, S., Maslehuddin, M., Al-Zahrani, M., Al-Juraifani, E., Alidi, S. and Al-Mehthel M. (2000). Performance evaluation of cement-based surface coatings, ACI Special Publication, 193.

Ba, M.F., Qian, C.X. and Wang H.(2013). Effects of specimen shape and size on water loss and drying shrinkage of cement-based materials, J Wuhan Univ Technol, 28: 733-740.

Banthia, N. and Mindess, S. (1989). Water permeability of cement paste, *Cement Concrete Res*, 19: 727-736.

Bakhshi, M., Mobasher, B. and Soranakom, C. (2012). Moisture loss characteristics of cement-based materials under early-age drying and shrinkage conditions, *Constr Build Mater*, 30: 413-425.

Baroghel-Bouny, V. (2007). Water vapour sorption experiments on hardened cementitious materials. Part II: Essential tool for assessment of transport properties and for durability prediction, *Cement Concrete Res*, 37: 438-454.

Baroghel-Bouny, V., Mainguy, M., Lassabatere, T. and Coussy, O. (1999). Characterization and identification of equilibrium and transfer moisture properties for ordinary and high-performance cementitious materials, *Cement Concrete Res*, 29: 1225-1238.

Baroghel-Bouny, V. (2007). Water vapour sorption experiments on hardened cementitious materials - Part I: Essential tool for analysis of hygral behaviour and its relation to pore structure, *Cement Concrete Res*, 37: 414-437.

Bentz, D.P. and Hansen, K.K. (2000). Preliminary observations of water movement in cement pastes during curing using X-ray absorption, *Cement Concrete Res*, 30: 1157-1168.

Bentz, D.P., Hansen, K.K., Madsen, H.D., Vallee, F. and Griesel, E.J. (2001). Drying/hydration in cement pastes during curing, *Mater Struct*, 34: 557-565.

Brocken, H.J.P., Spiekman, M.E., Pel, L., Kopinga, K. and Larbi, J.A. (1998). Water extraction out of mortar during brick laying: A NMR study, *Mater Struct*, 31: 49-57.

Daian, J.F. (1998). Condensation and isothermal water transfer in cement mortar Part I—Pore size distribution, equilibrium water condensation and imbibition, *Transport Porous Med*, 3: 563-589.

Faure, P., Caré, S., Po, C. and Rodts, S. (2005). An MRI-SPI and NMR relaxation study of drying–hydration coupling effect on microstructure of cement-based materials at early age, *Magnetic Resonance Imaging*, 23: 311-314.

Ho, C.K. and Webb, S.W. (2006). Gas transport in porous media, Springer.

Jennings, H.M. and Tennis, P.D. (1994). Model for the Developing Microstructure in Portland-Cement Pastes, *J Am Ceram Soc*, 77: 3161-3172.

Jennings, H.M., Bullard, J.W., Thomas, J.J., Andrade, J.E., Chen, J.J. and Scherer, G.W. (2008), Characterization and modeling of pores and surfaces in cement paste: correlations to processing and properties, *J Adv Concr Technol*, 6: 5-29.

Jensen, O.M. and Hansen, P.F. (2001) Water-entrained cement-based materials: I. Principles and theoretical background, *Cement Concrete Res*, 31: 647-654.

Kazemi Kamyab, M., Denarié, E., Brühwiler, E., Wang, B., Thiéry, M., Faure, P.F. and Baroghel-Bouny, V. (2012). Characterization of moisture transfer in UHPFRC-concrete composite systems at early age, Proceedings of the 2nd *International Conference on Microstructural-related Durability of Cementitious Composites*, 163.

Kim, J.K. and Lee, C.S. (1999). Moisture diffusion of concrete considering self-desiccation at early ages, *Cement Concrete Res*, 29: 1921-1927.

Koenders, E.A.B. *Simulation of volume changes in hardening cement-based materials*, Ph.D. thesis, Delft University of Technology, The Netherlands, 1997.

Li, M. and Li V.C. (2006). Behavior of ECC/concrete layer repair system under drying shrinkage conditions, *Proceedings of ConMat*, 5: 22-24.

Lukovic, M., Savija, B., Schlangen, E., Ye, G. and van Breugel, K. (2014) A modelling study of drying shrinkage damage in concrete repair systems, *Structural faults and repair conference 2014*, London, UK, The Electrochemical Society.

Lukovic, M. and Ye, G. (2015) Effect of Moisture Exchange on Interface Formation in the Repair System Studied by X-ray Absorption, *Materials*, 9: 2.

Martinola, G. and Sadouki, H. (1998). Combined experimental and numerical study to assess shrinkage cracking of cement-based materials, *International Journal for Restoration of Buildings and Monuments*, 4: 479-506.

Martinola, G., Sadouki, H. and Wittmann, F.H. (2001). Numerical model for minimizing risk of damage in repair system, *J Mater Civil Eng*, 13: 121-129.

McNamara, G.R. and Zanetti, G. (1988). Use of the Boltzmann equation to simulate lattice-gas automata, *Physical Review Letters*, 61: 2332.

Millington, R. and Quirk, J. (1961). Permeability of porous solids, *Transactions of the Faraday Society*, 57: 1200-1207.

Mindess, S., Young, J.F. and Darwin, D. (2003). *Concrete*, Prentice Hall.

Nurge, M.A., Youngquist, R.C. and Starr, S.O. (2010). Mass conservation in modeling moisture diffusion in multi-layer composite and sandwich structures, *Journal of Sandwich Structures and Materials*.

Nyame, B.K. *Permeability and Pore Structure of Hardened Cement Paste and Mortar*, Ph.D. thesis, King's College London, United Kingdom, 1979.

Oh, B.H and Cha, S.W. (2001). Realistic models for degree of hydration and moisture distribution in concrete at early age, Fourth International Conference on Fracture *Mechanics of Concrete and Concrete Structures*, 279-286.

Oh, B.H. and Cha, S.W. (2003). Nonlinear analysis of temperature and moisture distributions in early-age concrete structures based on degree of hydration, *Aci Mater J*, 100.

Powers, T.C. and Brownyard, T.L. (1946). Studies of the physical properties of hardened Portland cement paste, *ACI Journal Proceedings*, ACI.

Powers, T.C., Copeland, L., Hayes, J. and Mann, H. (1954). Permeablity of Portland Cement Paste, *ACI Journal proceedings*, ACI.

Prodanovic, M. and Bryant, S.L. (2006). A level set method for determining critical curvatures for drainage and imbibition, *Journal of Colloid and Interface Science*, 304: 442-458.

Ranaivomanana, H., Verdier, J., Sellier, A. and Bourbon, X. (2013). Prediction of relative permeabilities and water vapor diffusion reduction factor for cement-based materials, *Cement Concrete Res*, 48: 53-63.

Richards, L.A. (1931). Capillary conduction of liquids through porous mediums, *Physics-J Gen Appl P*, 1: 318-333.

Saeidpour, M. and Wadsö, L. (2015). Moisture equilibrium of cement based materials containing slag or silica fume and exposed to repeated sorption cycles, *Cement Concrete Res*, 69: 88-95.

Samson, E., Marchand, J., Snyder, K.A. and Beaudoin, J.J. (2005). Modeling ion and fluid transport in unsaturated cement systems in isothermal conditions, *Cement Concrete Res*, 35: 141-153.

Saricimen, H., Maslehuddin, M., Iob, A. and Eid, O.A. (1996). Evaluation of a surface coating in retarding reinforcement corrosion, *Constr Build Mater*, 10: 507-513.

Šelih, J., Sousa, A.C. and Bremner, T.W. (1996). Moisture transport in initially fully saturated concrete during drying, *Transport Porous Med*, 24: 81-106.

Shi, X., Xie, N., Fortune, K. and Gong, J. (2012). Durability of steel reinforced concrete in chloride environments: An overview, *Constr Build Mater*, 30: 125-138.

Shimomurat, T. and Maekawa, K. (1997). Analysis of the drying shrinkage behaviour of concrete using a micromechanical model based on the micropore structure of concrete, *Mag Concrete Res*, 49: 303-322.

Snyder, K.A. and Bentz, D.P. (2004). Suspended hydration and loss of freezable water in cement pastes exposed to 90% relative, *Cement Concrete Res*, 34 (11), 2045-2056.

Szymkiewicz, A. (2012). *Modelling water flow in unsaturated porous media: accounting for nonlinear permeability and material heterogeneity*, Springer Science & Business Media.

Taylor, H.F. (1987). A method for predicting alkazi ion concentrations in cement pore solutions, *Advances in Cement Research*, 1: 5-17.

Tennis, P.D. and Jennings, H.M. (2000). A model for two types of calcium silicate hydrate in the microstructure of Portland cement pastes, *Cement Concrete Res*, 30: 855-863.

Van Genuchten, M.T. (1980). A closed-form equation for predicting the hydraulic conductivity of unsaturated soils, *Soil science society of America journal*, 44: 892-898.

Van Breugel, K. *Simulation of hydration and formation of structure in hardening cement-based materials*, Ph.D. thesis, Delft University of Technology, The Netherlands, 1991.

Wiederhold, P.R. (1997). *Water vapor measurement: methods and instrumentation*, CRC Press.

Xi, Y.P., Bazant, Z.P. and Jennings, H.M. (1994). Moisture Diffusion in Cementitious Materials - Adsorption-Isotherms, *Adv Cem Based Mater*, 1: 248-257.

Zalzale, M. and McDonald, P. (2012). Lattice Boltzmann simulations of the permeability and capillary adsorption of cement model microstructures, *Cement Concrete Res*, 42: 1601-1610.

Zhang, J., Qi, K. and Huang, Y. (2009). Calculation of moisture distribution in early-age concrete, *Journal of engineering mechanics*, 135: 871-880.

Zhang, J., Wang, J. and Gao, Y. (2016). Moisture movement in early-age concrete under cement hydration and environmental drying, *Mag Concrete Res*, 68: 391-408.